ELSEVIER

Biochimica et Biophysica Acta 1369 (1998) 152–158

BIOCHIMICA ET BIOPHYSICA ACTA
BBA

Permeation of redox species through a cell membrane of a single, living algal protoplast studied by microamperometry

Tomoyuki Yasukawa [a], Isamu Uchida [a,b], Tomokazu Matsue [a,b,*]

[a] *Department of Applied Chemistry, Graduate School of Engineering, Tohoku University, Aramaki, Aoba, Sendai 980-77, Japan*
[b] *Center for interdisciplinary Research, Tohoku University, Aramaki, Aoba, Sendai 980-77, Japan*

Received 3 June 1997; revised 5 September 1997; accepted 12 September 1997

Abstract

Permeation of several redox species through a cell membrane of a single algal protoplast (radius 100 μm) was investigated by amperometry with a Pt microdisk electrode (disk radius, 6.5 μm) located near the membrane. The redox current observed at the microelectrode decreased as the microelectrode approached the cell membrane since the membrane acted as a barrier for diffusion of redox species from bulk to the microelectrode. Permeability coefficient (P_m) of the protoplast membrane was determined by the quantitative analysis of the variation of the redox current with microelectrode-membrane distance using digital simulation. The P_m values for $Fe(CN)_6^{4-}$, $Fe(CN)_6^{3-}$, $Co(phen)_3^{2+}$, ferrocenyl methanol(FMA) and *p*-hydroquinone(QH_2) were $\leq 1.0 \times 10^{-4}$, $\leq 1.0 \times 10^{-4}$, 1.0×10^{-3}, 5.0×10^{-3} and 2.0×10^{-2} cm/s, respectively. Using these P_m values, the concentration changes inside a model cell and chloroplast were theoretically calculated. © 1998 Elsevier Science B.V.

Keywords: Permeability coefficient; Microamperometry; Single cell; Microelectrode; Algal protoplast

1. Introduction

The understanding of how molecules move across a membrane of a living cell is vital for elucidating the function of a membrane. Previous studies of molecular transport and diffusion across membranes have revealed that the permeability coefficient (P_m) of synthetic membranes to molecules or ions is roughly proportional to the solubility of these species into hydrocarbons such as *n*-decane [1–8]. It is, however, difficult to determine accurate P_m values to hydrophobic species which can diffuse rapidly across the membrane, since the unstirred solution with the P_m value equivalent to 10^{-3} cm/s is present next to the membrane. The determination of large P_m values for hydrophobic species requires a technique to monitor accurately the change in concentration in the vicinity region of the membrane [9,10]. We previously proposed a microamperometric method [11] to determine the P_m values of a synthetic membrane to hydrophobic species. In this method, a microelectrode with a tip size on a micrometer scale was placed inside the unstirred solution layer to monitor the change in concentration of hydrophobic species permeated from the other side of the solution.

Microamperometric measurements afford electrochemical information in localized space on the scale of the electrode size and have been applied for the investigation of cellular processes such as cate-

* Corresponding author: Fax: +81 22 217 7293; E-mail: matsue@est.che.tohoku.ac.jp

PII S0005-2736(97)00220-4

cholamine release [12,13], NO release [14], photosynthesis [15,16], respiration [17], and oxidative stress [18]. In the present study, the microamperometric measurement was used for quantitative analysis of the permeation of several redox species through a cell membrane of a single protoplast. When a microelectrode is in the bulk solution, a steady-state diffusion region of the redox species expands semi-spherically into the solution and gives a steady-state redox current (i_d) expressed by

$$i_d = 4nFDCa \quad (1)$$

where n is the number of electrons involved in the redox reaction, F is the Faraday constant, D is the diffusion coefficient of redox species, C is the bulk concentration of redox species, a is the electrode radius exposed to the solution (Fig. 1(a)). When the microelectrode is placed close to a membrane which influences the formation of the semi-spherical diffusion region, the redox current becomes lower than that observed in the bulk solution (Fig. 1(b) and (c)). Since the decrease in the redox current correlates with the permeability of the membrane to redox species, the quantitative analysis of the phenomenon affords the P_m values for redox species to pass through the membrane.

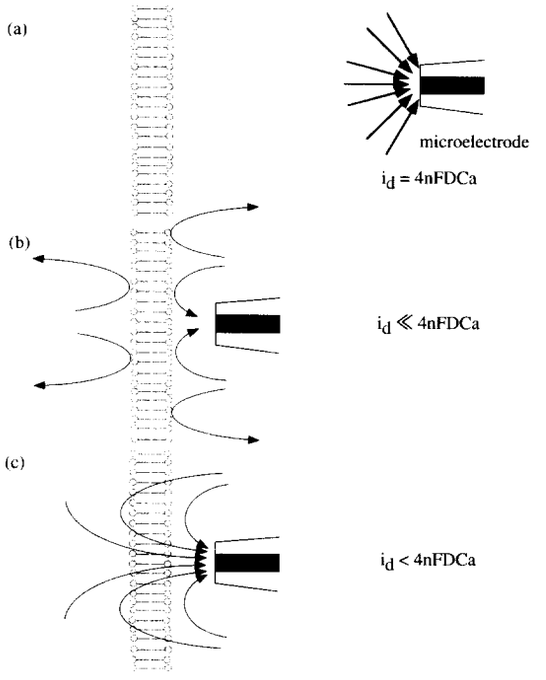

Fig. 1. Redox response at a microelectrode. In the bulk solution, a steady-state current (Eq. (1)) is observed (a) When the microelectrode is placed close to a membrane, the redox response becomes lower than that in the bulk solution. The response depends greatly on the permeability of the membrane (b) impermeable; (c) permeable. These phenomena can be used for determining the permeability coefficient (P_m).

We report here the P_m values of a cell membrane of an intact, single protoplast to several redox species. Cellular energy production by respiration and photosynthesis are based on biological electron-transport. Thus, the interaction of redox species added to outside solution with the intracellular electron-transport process has been frequently studied to clarify cellular activities and functions [19]. To view real feature of the interaction, it is essential to understand the permeation of redox species through an intact cell membrane since the membrane sometimes acts as a barrier for the permeation of redox species and might limit the intracellular electron-transfer. In relation to this aspect, we also theoretically investigated how the intracellular concentration of redox species changes as a function of time using the P_m values determined in the present study.

2. Materials and methods

GR-grade $K_4Fe(CN)_6$, $K_3Fe(CN)_6$, *p*-hydroquinone (QH_2) and *p*-benzoquinone (BQ) were purchased from Wako Pure Chemicals, and used without further purification. Ferrocenylmethanol (FMA) was synthesized by reduction of ferrocenecarboxyaldehyde (Aldrich) with $NaBH_4$ and recrystallized twice from *n*-hexane. $Co(phen)_3(ClO_4)_2$ was synthesized according to the literature [20]. Protoplast with a radius of 100 μm was made from marine alga *Bryopsis plumosa* by the method reported previously [21] in a synthetic artificial sea water containing 480.2 mM NaCl, 2.3 mM $NaHCO_3$, 11.1 mM $CaCl_2$ and 83.8 mM $MgCl_2$. The permeability measurements were started about 20 min after the protoplast was prepared. The measurements were usually completed within 1 h. All the aqueous solutions were prepared with distilled and deionized water by AQUARIUS GS-200 (Advantec) and Milli-Q Jr (Millipore).

The working electrode was prepared as follows. A Pt wire (7.5 μm in radius) was slightly etched elec-

trochemically in a $NaNO_3$ saturated aqueous solution to clean the surface. The etched wire was inserted into a glass capillary and the tip region was thermally fused in vacuo. Then, the tip was carefully polished with a diamond grinder (# 5000) on a turntable (Narishige, Model EG-6) to give a disk-shaped Pt electrode. The radius of the Pt disk was determined from the steady-state oxidation current of $Fe(CN)_6^{4-}$ in a voltammogram and found to be 6.5 μm [22]. From microscopic measurements, the tip radius including insulating glass was 12 μm. The measurements were carried out by a two-electrode system with Ag/AgCl as a counter/reference electrode. Redox current was measured by amperometry at 0.00 V for $Fe(CN)_6^{3-}$, 0.50 V for $Fe(CN)_6^{4-}$, $Co(phen)_3^{2+}$ and FMA, and 0.80 V for QH_2. Before the measurements, a cleaning pulse (1.0 V for 0.4 s, −1.0 V for 0.4 s) was applied to the microelectrode. All measurements were performed at 25°C in a shield box. The position of the microelectrode was controlled by a three-dimensional manipulator system (Shimazu, MMS-77) under a microscope (Nikon, DIAPHOT 300). The microelectrode was placed close to the protoplast membrane with the disk surface aligned to be parallel to the membrane surface. The image was monitored on a CRT (NEC, PC-TV 455) through a CCD color video camera (Sony, DXC-107A). Redox current was amplified with a current amplifier (Nihon Kohden, CZE-2300). Control of the electrode potential and data acquisition was performed with a personal computer (NEC 98note, SX/E) with a 12-bit AD/DA board (AB 98-57B, Adtec).

The digital simulation with the fast quasi explicit finite difference (FQEFD) method [23,24] was used to obtain the theoretical response at the microelectrode. We considered the protoplast membrane as a flat surface with an uniform P_m value. To save the computation time the axial symmetrical grid model was used for the simulation. The details of the simulation was described in the previous paper [25]. We calculated the change in the oxidation current after the applied potential was stepped from sufficiently negative to sufficiently positive value where the electrode reaction was determined only by the diffusion. The P_m values of the protoplast membrane to the redox species were determined by comparing the experimentally-observed responses with the calculated ones [25,26].

We also used explicit finite difference method to simulate the permeation and diffusion of redox species into a spherical model protoplast having a small concentric sphere (1:10 in size) inside the model protoplast. The small sphere was considered as a model chloroplast. In this simulation, the spherical diffusion was considered with exponentially-expanded (outside the cell) and uniformly-divided (inside the cell) space grids. The initial and boundary conditions are as follows:

$t = 0$, outside the cell $C = C^*$; inside the cell $C = 0$

$t > 0$, bulk solution $C = C^*$

cell and chloroplast membranes $f = P_m(C^{out} - C^{in})$

where C^* is the bulk concentration, C^{out} is the outside concentration at the membrane, C^{in} is the inside concentration at the membrane, f is the flux, The calculation was carried out using a dimensionless time parameter, Dt/r^2, and a permeability parameter, $P_m r/D$ (r: radius of the cell).

The diffusion coefficients of $Fe(CN)_6^{4-}$ (6.5×10^{-6} cm^2/s) and $Fe(CN)_6^{3-}$ (7.6×10^{-6} cm^2/s) are taken from a literature [27]. The diffusion coefficients of $Co(phen)_3^{2+}$, FMA, QH_2 and BQ were determined by potential-step chronoamperometry and found, respectively, to be 4.7×10^{-6}, 7.0×10^{-6}, 6.2×10^{-6} and 6.2×10^{-6} cm^2/s. These values were used for quantitative analysis of the microamperometric behavior.

3. Results and discussion

We investigated the permeation of five redox species, $Fe(CN)_6^{4-}$, $Fe(CN)_6^{3-}$, $Co(phen)_3^{2+}$, FMA and QH_2 through the algal protoplast membrane. Fig. 2 shows the variations of oxidation currents of 1.0 mM $Fe(CN)_6^{4-}$ and 1.0 mM QH_2 at the microelectrode as the electrode stepwise approaches a single protoplast. The electrode potential was held at 0.50 V vs. Ag/AgCl for $Fe(CN)_6^{4-}$ and 0.80 V vs. Ag/AgCl for QH_2 where the electrode reaction was limited by diffusion of $Fe(CN)_6^{4-}$ and QH_2. The oxidation current depends on the position of the microelectrode. When the microelectrode is placed close to the protoplast membrane, the observed response of $Fe(CN)_6^{4-}$ is much smaller than observed in the bulk solution.

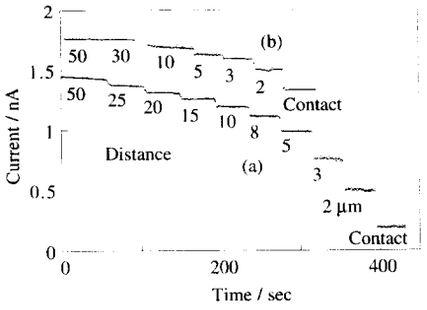

Fig. 2. Responses of oxidation currents for (a) $Fe(CN)_6^{4-}$ and (b) QH_2 at various tip-protoplast distances. The oxidation currents decrease as the microelectrode approaches stepwide the protoplast membrane. The decrease is eminent for $Fe(CN)_6^{4-}$, suggesting that $Fe(CN)_6^{4-}$ is less permeable to the membrane than QH_2.

This finding clearly indicates that the protoplast membrane acts as a barrier for $Fe(CN)_6^{4-}$ to diffuse from the bulk solution to the electrode surface and, therefore, the permeability of the protoplast membrane for the passage of $Fe(CN)_6^{4-}$ is small. On the other hand, the oxidation current of QH_2 decreased only slightly when the tip approached the cell membrane, suggesting that QH_2 can permeate the membrane in the time scale investigated.

The response at the microelectrode shows a staircase-shape synchronized with the movement of the microelectrode. It should be noted here that the change in the oxidation current response in each step (ca. 40 s) is very small. The decrease of the current from 5–40 s at 2 μm distance is less than 5%. The above finding demonstrates that the diffusion of $Fe(CN)_6^{4-}$ also rapidly reaches steady-state similar to in bulk solution, although the diffusion region is not spherical due to inhibition of free diffusion by the protoplast membrane. The digital simulation of the potential-step amperometry reproduces this situation. When the tip of a microelectrode (6.5 μm disk-radius, 12 μm tip-radius) is placed 2.0 μm away from an impermeable membrane, the calculated oxidation current reaches quasi-steady state value in 10 s after the potential is stepped to a sufficiently positive value. The decrease of the oxidation current in the subsequent 10–40 s is less than 1%. Therefore, we adopted the responses at 30 s in each step for quantitative investigation of permeation of redox species through a cell membrane.

Fig. 3 show the plots of the redox current for $Fe(CN)_6^{4-}$, $Fe(CN)_6^{3-}$, $Co(phen)_3^{2+}$, FMA and QH_2 against the electrode–protoplast membrane distance. The oxidation currents for $Fe(CN)_6^{4-}$, $Fe(CN)_6^{3-}$ and $Co(phen)_3^{2+}$ decrease markedly when the distance is below 15 μm. In the bulk solution, the formation of a steady-state, semi-spherical diffusion region with the electrode dimension gives a steady-state redox current expressed by Eq. (1). When the electrode–membrane distance is within the electrode dimension, the cell membrane influences the formation of the diffusion region. The decrease in the response within 15 μm is a consequence that the membrane blocks the spherical diffusion and permeation of $Fe(CN)_6^{4-}$, $Fe(CN)_6^{3-}$ and $Co(phen)_3^{2+}$. The decrease in the oxidation current of FMA and QH_2 was, on the other hand, small compared to that observed for $Fe(CN)_6^{4-}$. The cell membrane dose not obstruct severely the diffusion of FMA and QH_2 and, therefore, FMA and QH_2 can easily permeate the membrane compared to $Fe(CN)_6^{4-}$.

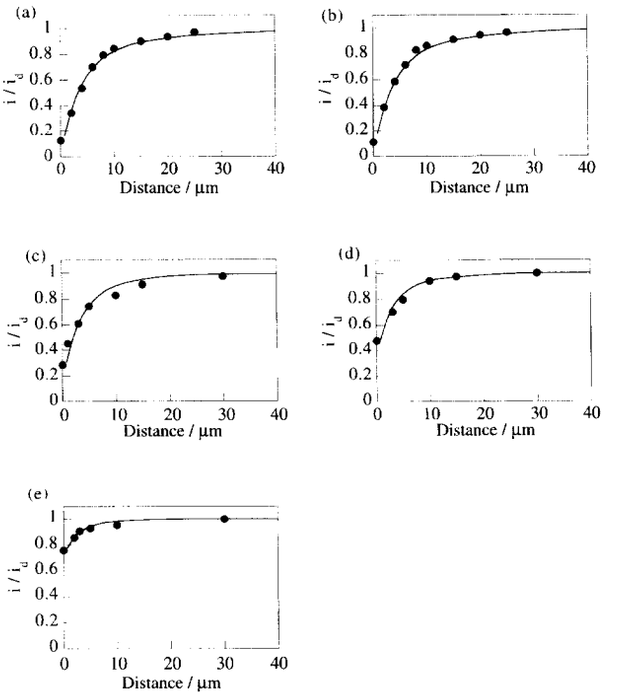

Fig. 3. Variations of redox current (relative) as a function of tip-protoplast membrane distance. Redox species: (a) $Fe(CN)_6^{4-}$, (b) $Fe(CN)_6^{3-}$, (c) $Co(phen)_3^{2+}$, (d) FMA, (e) QH_2. Solid curves: Theoretical for P_m = (a, b) 1.0×10^{-4}, (c) 1.0×10^{-3}, (d) 5.0×10^{-3}, (e) 2.0×10^{-2} cm/s.

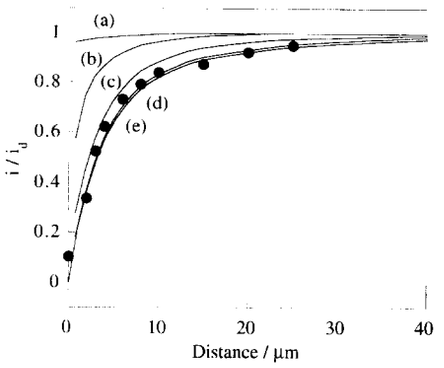

Fig. 4. Theoretical relative current as a function of tip-protoplast membrane distance for various permeability coefficients (P_m's). P_m value (cm/s): (a) 1.0×10^{-1}, (b) 1.0×10^{-2}, (c) 1.0×10^{-3}, (d) 1.0×10^{-4}, (e) 1.0×10^{-5}. Redox species: 1.0 mM $Fe(CN)_6^{4-}$. The current vs. distance profile depends on the P_m value when $10^{-1}\,cm/s \geq P_m \geq 10^{-4}\,cm/s$. This theoretical response was used for determination of P_m values of the redox species by the curve-fitting method. Closed circles: Experimental data when the microelectrode was moved to an impermeable glass substrate. This experimental plot fits well with the theoretical ones for $P_m \leq 10^{-4}\,cm/s$.

We calculated the electrochemical responses at a microelectrode by digital simulation using parameters comparable to the experimental conditions to determine the permeability coefficients (P_m's) of the protoplast membrane to these redox species. Fig. 4 shows the relative current vs. distance plots obtained by the simulation, together with the experimentally-observed response of $Fe(CN)_6^{4-}$ when the microelectrode moved to a glass substrate which is impermeable to $Fe(CN)_6^{4-}$. The obvious decrease in the response is theoretically observed when $P_m \leq 0.1\,cm/s$. The theoretical current vs. distance plot shows no longer change when $P_m \leq 10^{-4}\,cm/s$. The experimental data of $Fe(CN)_6^{4-}$ for the impermeable substrate accords well with the theoretical plots for $P_m \leq 10^{-4}\,cm/s$. Therefore, it is difficult to determine the P_m values for less permeable species ($P_m \leq 10^{-4}\,cm/s$) by comparing the experimental data with theoretical ones. The shape of the plot depends greatly on the P_m value in the range, $10^{-4}\,cm/s \leq P_m \leq 10^{-1}\,cm/s$. In this region, the P_m values of the membrane can be determined by curve-fitting with the P_m value as an adjusting parameter. The calculated current vs. distance curves which properly accord with the experimental data are shown in Fig. 3. The theoretical curves with $P_m = 1.0\times10^{-3}$, 5.0×10^{-3} and $2.0\times10^{-2}\,cm/s$ give excellent fittings with the experimental data for $Co(phen)_3^{2+}$, FMA and QH_2, respectively. Since experimental data for $Fe(CN)_6^{4-}$ and $Fe(CN)_6^{3-}$ (Fig. 3(a) and (b)) are almost identical to that for the impermeable case shown in Fig. 4, the most that can be said is that the P_m values for $Fe(CN)_6^{4-}$ and $Fe(CN)_6^{3-}$ are below $1.0\times10^{-4}\,cm/s$ and the cell membrane is practically impermeable to these species. The results are summarized in Table 1.

The permeability of a cell membrane is closely related with hydrophobicity, mass and total charge of the species to permeate. The permeability of a cell membrane to QH_2 is large because it is comparatively small and present in the fully protonated neutral form under the experimental conditions (pKa of QH_2, 9.96 [28]). FMA also permeates easily the protoplast membrane. In contrast, the protoplast membrane is almost impermeable to charged, hydrophilic species such as $Fe(CN)_6^{4-}$ and $Fe(CN)_6^{3-}$. Slight permeation of $Co(phen)_3^{2+}$ through the cell membrane was observed probably because this complex is surrounded by organic aromatic rings. In addition, the electrostatic interaction between the positively-charged complex and negatively-charged membrane might help the permeation of $Co(phen)_3^{2+}$. We also investigated the permeation of *p*-benzoquinone (BQ). Qualitatively, BQ also permeates rapidly the protoplast membrane as does QH_2. It is, however, difficult to determine the accurate P_m value for BQ, since the permeated BQ interacts with photosynthetic and respiratory electron-transfer chains. The

Table 1
Permeation parameters of redox species through the protoplast membrane

Redox species	D (cm^2/s)	P_m(cm/s)[a]	$P_m r/D$[b]	t(s)[c]
$Fe(CN)_6^{4-}$	6.5×10^{-6}	$\leq 1.0\times10^{-4}$	≤ 0.15	≥ 125
$Fe(CN)_6^{3-}$	7.6×10^{-6}	$\leq 1.0\times10^{-4}$	≤ 0.13	≥ 123
$Co(phen)_3^{2+}$	4.7×10^{-6}	1.0×10^{-3}	2.3	40
FMA	7.0×10^{-6}	5.0×10^{-3}	7.1	23
QH_2	6.2×10^{-6}	2.0×10^{-2}	32	24
BQ	6.2×10^{-6}	$\geq 1.0\times10^{-3}$	≥ 2.3	≤ 41

[a] P_m values were determined by the curve-fitting method.
[b] Dimensionless permeability; r, radius of the cell.
[c] Time required for the average concentration in the model chloroplast to reach 95% of the bulk solution ($r = 100\,\mu m$).

reduction current vs. distance plot for BQ suggests that $P_m \geq 5 \times 10^{-3}$ cm/s.

The numerous studies on intracellular energy production in chloroplasts and mitochondria have addressed electron-transfer between the energy-producing proteins and redox chemicals added to outside media. It is, therefore, important to know how rapidly the redox species in the outside media permeate through the cell and chloroplast (or mitochondrion) membranes to interact the redox proteins. Based on the permeability coefficients determined by the present microamperometric method, we have theoretical investigated the permeation phenomena through the cell and chloroplast membranes using a model cell. Our model cell is spherical with a small concentric sphere (1:10 in size) which is considered as a model chloroplast. We assumed that the permeability of the innersphere membrane was equal to that of the outersphere membrane.

Fig. 5 shows the variation of average concentration inside the model chloroplast as a function of the dimensionless time parameter, Dt/r^2, for the dimensionless permeability parameter, $P_m r/D = 0.1$, 1, 2, 5 and 10. The average concentration increases rapidly as the membrane permeability increases. If we adapt the parameters corresponding to the present experimental conditions ($r = 100\,\mu$m), the dimensionless values of $P_m r/D$ for $Co(phen)_3^{2+}$, FMA and QH_2 are 2.3, 7.1 and 32, respectively. Using these values, we have calculated the time ($t_{0.95}$) required for the average concentration in the model chloroplast to reach 95% of the bulk concentration after adding redox species to the outside solution. The $t_{0.95}$ values for $Co(phen)_3^{2+}$, FMA and QH_2 are, respectively, 40, 23 and 24 s. The calculation results are also listed in Table 1. Since the permeability coefficients of the protoplast membrane to $Fe(CN)_6^{4-}$ and $Fe(CN)_6^{3-}$ are below 1.0×10^{-4} cm/s, Table 1 lists only the lower limits of $t_{0.95}$ for these species. For comparison, the $t_{0.95}$ values for $P_m = 1 \times 10^{-5}$ and 1×10^{-6} cm/s are 1×10^3 and 1×10^4 s, respectively.

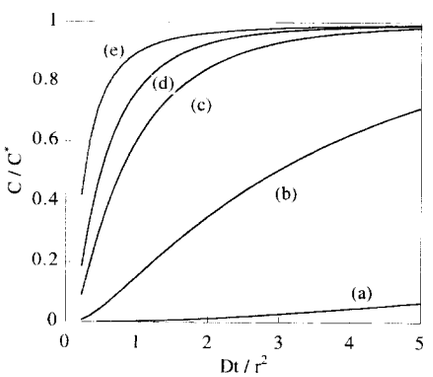

Fig. 5. Change of average concentration in a model chloroplast as a function of the dimensionless time parameter, Dt/r^2. $P_m r/D$: (a) 0.01, (b) 0.1, (c) 0.5, (d) 1, (e) 5. Calculation was carried out using a spherical model cell with a small concentric chloroplast (1:10 in size) based on the assumption that the permeability of the chloroplast membrane was equal to that of the cell membrane.

In the present study, we have used microamperometric method to determine the permeability coefficients of a membrane of an intact and single cell to several redox species. The redox response at a microelectrode decreases as the electrode approaches the membrane surface since the membrane acts as a barrier for diffusion of redox species from bulk to electrode surface. The quantitative analysis of these phenomena using digital simulation gives permeability coefficients. The present results demonstrate that the cell membrane is highly permeable to QH_2, BQ and FMA, and moderately permeable to $Co(phen)_3^{2+}$, and almost impermeable to $Fe(CN)_6^{4-}$ and $Fe(CN)_6^{3-}$. For QH_2 and FMA, the average concentration inside the cell (radius, 100 μm) reaches 95% of bulk concentration within 20 s. Many laboratories, including ours, have reported intracellular electrochemical measurements using microelectrodes to monitor intracellular reactions. However, the insertion of microelectrodes physically injures the cell and triggers undesired intracellular reactions. It is, therefore, important to evaluate the permeability of a cell membrane to redox species by the extracellular measurements to understand intrinsic membrane phenomena. Based on the above results, we will be able to conduct kinetic investigation about the interaction of the permeated redox species with photosynthesis and respiration chains.

Acknowledgements

This work was partly supported by Grants-in-Aid for Scientific Research A (08555198) and for Scientific Research on Priority Area of "Electrochemistry of Ordered Interfaces" (09237106) from the Ministry of Education, Science and Culture, Japan.

References

[1] J.M. Diamond, Y. Katz, J. Membr. Biol. 17 (1974) 121–154.
[2] R.F. Flewelling, W.L. Hubbell, Biophys. J. 49 (1986) 531–540.
[3] H. Hauser, D. Oldani, M.C. Phillips, Biochemistry 12 (1973) 4507–4517.
[4] A. Walter, J. Gutknecht, J. Membr. Biol. 77 (1984) 255–264.
[5] A. Walter, J. Gutknecht, J. Membr. Biol. 90 (1986) 207–217.
[6] J. Gutknecht, A. Walter, Biochim. Biophys. Acta 685 (1982) 233–240.
[7] J. Gutknecht, A. Walter, Biochim. Biophys. Acta 641 (1981) 183–188.
[8] J. Gutknecht, A. Walter, Biochim. Biophys. Acta 644 (1981) 153–156.
[9] Y.N. Antonenko, A.A. Bulychev, Biochim. Biophys. Acta 1070 (1991) 279–282.
[10] Y.N. Antonenko, A.A. Bulychev, Biochim. Biophys. Acta 1070 (1991) 474–480.
[11] H. Yamada, T. Matsue, I. Uchida, Biochem. Biophys. Res. Commun. 180 (1991) 1330–1334.
[12] R.M. Wightman, S. Hochstetler, D. Michael, E. Travis, Electrochem. Soc. Interface (Fall, 1996) 22–26.
[13] R.M. Wightman, L.J. May, A.C. Michael, Anal. Chem. 60 (1988) 769A–779A.
[14] T. Malinski, Z. Taha, Nature 358 (1992) 676–678.
[15] T. Matsue, S. Koike, I. Uchida, Biochem. Biophys. Res. Commun. 197 (1993) 1283–1287.
[16] T. Matsue, S. Koike, T. Abe, T. Itabashi, I. Uchida, Biochim. Biophys. Acta 1101 (1992) 69–72.
[17] Y.Y. Lau, T. Abe, A.G. Ewing, Anal. Chem. 64 (1992) 1702–1705.
[18] S. Arbault, P. Pantano, J.A. Jankowski, M. Vuillaume, C. Amatore, Anal. Chem. 67 (1995) 3382–3390.
[19] T. Ikeda, T. Kurosaki, K. Takayama, K. Kano, Anal. Chem. 68 (1996) 192–198.
[20] F.A. Cotton, Inorganic Synthesis, vol. 13, McGraw-Hill, New York, 1972, pp. 211–212.
[21] M. Tatewaki, K. Nagata, J. Phycol. 6 (1970) 401–403.
[22] R.M. Wightman, Anal. Chem. 53 (1981) 1125A–1134A.
[23] S.W. Feldberg, J. Electroanal. Chem. 290 (1990) 49–65.
[24] S.W. Feldberg, J. Electroanal. Chem. 127 (1981) 1–10.
[25] H. Shiku, T. Takeda, H. Yamada, T. Matsue, I. Uchida, Anal. Chem. 67 (1995) 312–317.
[26] H. Yamada, H. Shiku, T. Matsue, I. Uchida, Bioelectrochem. Bioenerg. 33 (1994) 91–93.
[27] D.T. Sawyer, J.L. Roberts, Experimental Electrochemistry for Chemists, Wiley, New York, 1974, p. 77.
[28] H.H. Willard, L.M. Lynne Jr., A.D. John, Instrumental Methods of Analysis, D. Van Nostrand Company, New York, 1965, p. 765.